http://dx.doi.org/10.21577/0103-5053.20190275

J. Braz. Chem. Soc., Vol. 31, No. 6, 1101-1109, 2020
Printed in Brazil - ©2020 Sociedade Brasileira de Química

Article

Simultaneous Transfer of Na^+, K^+, and Fe^{2+} Ions During Salting of Precooked Mushroom (*Agaricus bisporus*): Mathematical Modeling, Optimization and Experimental Validation

Mirian S. P. Bordin,[a] Hágata Cremasco,[a] Diego Galvan,[a] Marco A. J. Clemente,[a] Evandro Bona,[b] Ana Carolina G. Mantovani[c] and Dionisio Borsato[,a]*

[a]*Departamento de Química, Universidade Estadual de Londrina, 86057-970 Londrina-PR, Brazil*

[b]*Programa de Pós-Graduação em Tecnologia de Alimentos, Universidade Tecnológica Federal do Paraná, 87301-899 Campo Mourão-PR, Brazil*

[c]*Departamento de Física, Universidade Estadual de Londrina, 86057-970 Londrina-PR, Brazil*

The champignon mushroom has no antinutritional factors that can affect iron bioavailability. It is considered a functional food and can provide health benefits by presenting bioactive components. The simultaneous transfer of Na^+, K^+ and Fe^{2+} in the pre-cooked mushroom (*Agaricus bisporus*) was modeled and simulated by the finite element method (FEM). The Biot number, cross and main diffusion coefficients were determined by the super modified simplex optimization method by minimizing the percentage errors. The errors between experimental and simulated data were 5.66% for NaCl, 5.36% for KCl and 8.26% for Fe^{2+} in the static brine and 3.11% for NaCl, 3.30% for KCl and 15.34% for Fe^{2+} in stirred brine. With the obtained model, it was possible to verify the influence of the film formed on the surface of the mushroom during the diffusion of ions, as well as the increase of ferrous ion adsorption when using the salting system with stirring.

Keywords: diffusion, iron, adsorption, finite element method, simplex optimization

Introduction

Iron is an essential mineral for human life due to redox reactions and transport of oxygen throughout the body.[1] It is estimated that 60% of the world population has some iron deficiency, which can cause diseases such as anemia, glossitis, angular stomatitis, koilonychia, blue sclera and esophageal web.[1,2]

Iron deficiency can often be caused by inadequate food intake and/or poor mineral availability. Therefore, there is an interest in increasing iron bioavailability from fortification, food enrichment and dietary supplementation.[1,3]

Iron bound to organic compounds such as amino acids, peptides and proteins, have greater bioavailability than free mineral because it forms stable and neutral complexes, protecting the micronutrient from chemical reactions that occur during the digestive process, ensuring its gastrointestinal solubility until absorption.[4,5] According to Regula *et al*.,[6] edible mushrooms do not have antinutritional factors that can affect the bioavailability of iron, so they could be enriched with this element.

The mushroom is a source of vitamin C, B1, B2, biotin, niacin, minerals and dietary fiber. On dry basis, its macronutrient composition is high, has a low caloric value, with a high protein content.[7] In addition, mushrooms are considered functional foods and can provide health benefits, i.e., leading to lower cancer incidence by presenting bioactive compounds, especially glucans, ergosterol, lecithins, and some immunomodulatory amino acids as arginine and glutamine.[8,9]

However, the mushroom is a food with high perishability as a result of its high moisture content. So, in order to increase its useful life, it can be subjected to conservation processes. The brine is one of the oldest methods of food preservation, in which the sodium chloride has antimicrobial function.[10] Although NaCl is essential for human health, excessive sodium intake has been related to hypertension.[11] Thus, potassium chloride is a suitable partial substitute for sodium chloride, which added in appropriate proportions, does not cause major sensory changes in the food.[12-14]

*e-mail: dborsato@uel.br

When several solutes are transferred from a liquid to a solid is necessary to know the Biot number as well as the main and cross diffusion coefficients, since the cross coefficient indicates the influence of one solute on the flow of the other solute.[15] To evaluate all these variables at the same time, multicomponent simulation is the most recommended.

The finite element method (FEM) is used to solve differential equations using a variational formulation or residual weight procedure, where a partial differential equation is transformed into a system of ordinary differential equations for a time dependent problem.[16] Several authors[17,18] have used finite element simulation coupled with optimization methods and desirability functions to determine mass transfer parameters.

The aim of this work was to simulate and model Na^+, K^+ and Fe^{2+} transfer during champignon mushroom salting, in static and stirred brine, using the finite element method with simplex optimization, to verify the transfer rates and the influence of the film formed on the mushroom surface during salt diffusion.

Experimental

Sample preparation

Champignon mushrooms (*Agaricus bisporus*) were purchased in a supermarket. Mushroom preparations followed the techniques recommended by Bordin *et al.*[17] and Gomes and Silva.[19]

Salting

It was prepared 10 L of brine with approximately 3% (m/v) of saline concentration, being 30% of potassium chloride (KCl, Synth, Diadema, Brazil), 69% of sodium chloride (NaCl, Panreac, Barcelona, Spain) and 1% of ferrous chloride (Sigma-Aldrich, St. Louis, USA).

The diffusion experiment was carried out in static and stirred solution, in a closed container in order to avoid evaporation, at 20 ± 1 °C during the whole process. In the experiment with stirred solution, a pump with a circulation flow of 520 L h^{-1} was used.

Determination of sodium, potassium and iron

After moisture determination, the samples were prepared for sodium, potassium and iron determination according the methodology described by Bordin *et al.*[17] The aliquots of the filtered solutions were analyzed by atomic emission (Micronal photometer, B-462, São Paulo, Brazil), with air pressure of 0.8 kgf cm^{-2}, air pump pressure of 1.5 kgf cm^{-2} using butane gas to quantify the sodium and potassium contents.[17]

The concentrations of NaCl and KCl salts in the mushroom were determined in the aqueous phase using the concentration units g 100 $g^{-1}_{(NaCl + KCl + Fe^{2+} + water)}$, and the Fe^{2+} concentration in the mushroom was determined by adsorbed brine g 100 $mL^{-1}_{(NaCl + KCl + Fe^{2+} + water)}$.

To quantify iron content, aliquots of the filtered solutions were analyzed on the flame atomic absorption spectrometer (FAAS, AA-7000, Shimadzu®, Kyoto, Japan). The flame composition used was air/acetylene with a flow rate of 15 L min^{-1} and 2.0 mL min^{-1}, respectively. A hollow cathode lamp was used as the radiation source of the Photron Hollow Cathode Lamps (Plainview, NY, USA) operated at 12.0 mA and iron wavelength of 248.33 nm. A deuterium lamp was used for background correction.

Adsorption of Fe^{2+} in the mushroom

The Fe^{2+} has affinity for functional groups compound as carbohydrates, fibers, amino acids, peptides and proteins, which constitute the matrix of the studied biosolid, enabling the formation of chelates.[5]

Mushroom adsorption isotherms were obtained by varying the initial concentration of ferrous ion in a batch processing at a constant temperature of 20 ± 1 °C, without stirring, with a contact time of 72 h. The volume of the solution used was 10 times larger than the volume occupied by the mushroom. In each polyethylene container, the pre-cooked mushroom of approximately 10.0 ± 0.4 g was immersed in brine containing 3% salts, being 30% of potassium chloride and 70% of sodium chloride at pH 4.5 ± 0.1, varying only the iron concentration from 10 to 200 mg L^{-1}. The levels of iron adsorbed on the mushroom were determined by the FAAS, and for the final Fe^{2+} solution concentration calculations the equation 1 was used.[20]

$$q_e = \frac{(C_0 - C_t)V}{m} \quad (1)$$

where: q_e is the amount adsorbed of Fe^{2+} (mg g^{-1}); C_0 is the initial concentration of Fe^{2+} solution (mg L^{-1}); C_t is the final concentration of Fe^{2+} solution; V is the volume of Fe^{2+} solution and m is the mushroom mass used (g).

Two models of adsorption isotherms were used to fit the experimental data.[21]

The Langmuir isotherm linear equation is represented by:

$$\frac{C_e}{q_e} = \frac{1}{q_m K_L} + \frac{C_e}{q_m} \quad (2)$$

where: C_e is the equilibrium concentration of the solute in the bulk solution (mg L^{-1}); q_m represents the maximum adsorptive capacity of the adsorbent (mg g^{-1}); K_L is the Langmuir adsorption constant that expresses the affinity between adsorbent and adsorbate and adsorption energy (L mg^{-1}).

The linear equation of the Freundlich isotherm is represented by the equation:[21]

$$\log q_e = \log K_F + \frac{1}{n}(\log C_e) \quad (3)$$

where: K_F is the Freundlich equilibrium constant and the parameter 1/n informs the linearity degree of the isotherm.

Mathematical modeling

Simulations of simultaneous mushroom salt transfers were solved by finite element method of the COMSOL Multiphysics® 5.2 software.[22] Two software interfaces were used. The "Transport of Diluted Species (tds)" was applied for the mass transfers of NaCl and KCl salts, and for the ferrous ion the "Transport of Diluted Species in Porous Media" was applied. The simulations were performed using the backward differentiation formula algorithm (BDF). The simulation procedure consisted of three steps: geometry construction, numerical mesh generation and mathematical model implementation in the software.

Geometry construction and mesh generation

From the average size of the mushrooms used in the mass transfer experiment, it was possible to create a biosolid through the internal computer-aided design (CAD) tool of the COMSOL software.[22] All simulations were made with a 3D geometry modeling in which the domain was subdivided into a fine mesh of tetrahedral finite elements consisting of 51,872 elements.

Mathematical modeling implementation

For the modeling, it was considered the simultaneous 3D mass transfer of three solutes in the mushroom, in which some simplifying considerations were made: (*i*) mass transfers of solutes occur in a three-dimensional matrix occupying a volume of $\Omega \subset R^3$, associated with a set of *x*, *y*, *z* coordinates; (*ii*) the diffusion coefficient and mass diffusivity are considered to be constant throughout the biosolid, regardless of the position and the immersion time of the solid; (*iii*) the predominant process in the mobility of NaCl and KCl salts is the diffusion; (*iv*) for ferrous ion mobility was considered the diffusion and adsorption governed by Langmuir law; (*v*) the density and porosity properties of the mushroom were considered constant over time; (*vi*) the process takes place under isothermal conditions of 20 ± 1 °C; (*vii*) sample contraction during the procedure was negligible; (*viii*) all the Fe^{2+} is maintained in its reduced form.

Thus, NaCl, KCl and Fe^{2+} concentrations were represented respectively by C_1 (*x*, *y*, *z*, t), C_2 (*x*, *y*, *z*, t) and C_3 (*x*, *y*, *z*, t) at a given point P (*x*,*y*,*z*) ∈ Ω and at a defined time t.

In the simulations, the physics of "Transport of Diluted Species (tds)" was used to describe the transports of NaCl and KCl in the fluid phase along the mushroom. Salt concentrations were determined based on Onsager equations (equations 4 and 5):[23]

$$\frac{\partial C_1}{\partial t} = D_{11}\nabla^2 C_1 + D_{12}\nabla^2 C_2 + D_{13}\nabla^2 C_3 \quad (4)$$

$$\frac{\partial C_2}{\partial t} = D_{21}\nabla^2 C_1 + D_{22}\nabla^2 C_2 + D_{23}\nabla^2 C_3 \quad (5)$$

where D_{11} and D_{22} are the main diffusion coefficients of NaCl and KCl, respectively; D_{12}, D_{21}, D_{13} and D_{23} are the cross-diffusion coefficients of the salts and $\nabla^2(.) = \nabla.\nabla(.)$ is the Laplacian operator.

According to the physics of COMSOL Multiphysics 5.2 software "Transport of Diluted Species in Porous Media",[22] the equations 6 and 7 were used to determine ferrous ion concentrations. These equations represent the ion transport in the fluid phase and the transfer to the solid phase (porous medium of the mushroom) by means of diffusion and adsorption mechanisms.

$$\left(\varepsilon_p + \rho K_{p3}\right)\frac{\partial C_3}{\partial t} + \left(c_3 - \rho_p c_{p3}\right)\frac{\partial \varepsilon_p}{\partial t} + D_{33}\nabla^2 C_3 + D_{31}\nabla^2 C_1 + D_{32}\nabla^2 C_2 = 0 \quad (6)$$

$$\rho_p = \frac{\rho}{\left(1-\varepsilon_p\right)} \quad (7)$$

where, ε_p represents the porosity of the solid; ρ_p the density of the solid; ρ the apparent density of the solid; K_{p3} the saturation constant of the isotherm; c_{p3} the maximum adsorbed concentration; D_{33} the effective diffusion coefficient of iron; D_{31} and D_{32} the cross-diffusion coefficients.

For the process modeling, the biosolid was characterized with apparent density of 1000.3 kg m^{-3} determined by the mass/volume ratio.

At the beginning of mass transfer processes, the initial concentrations of mushroom NaCl, KCl and Fe^{2+} are given by $C_{1,0}$, $C_{2,0}$ and $C_{3,0}$, according to equations 8, 9, and 10, respectively:

$$C_1(x, y, z, 0) = C_{1,0} \quad (8)$$
$$C_2(x, y, z, 0) = C_{2,0} \qquad x, y, z \in \Omega \quad (9)$$
$$C_3(x, y, z, 0) = C_{3,0} \quad (10)$$

Equations 11-13 account for the boundary conditions in the diffusion process.

$$\frac{\partial C_1(\pm R,t)}{\partial n} = \frac{h_m}{\lambda_m}\left[C_1 - C_{1,s}\right] \quad (11)$$

$$\frac{\partial C_2(\pm R,t)}{\partial n} = \frac{h_m}{\lambda_m}\left[C_2 - C_{2,s}\right] \quad x, y, z \in \partial\Omega,\ t > 0 \quad (12)$$

$$\frac{\partial C_3(\pm R,t)}{\partial n} = \frac{h_m}{\lambda_m}\left[C_3 - C_{3,s}\right] \quad (13)$$

where: h_m (m s^{-1}) is the mass transfer coefficient of the solute in the film formed around the mushroom; $\partial\Omega$ is the set of surface points that surrounds the mushroom; λ_m (m^2 s^{-1}) is the mass conductivity; $C_{1,s}$, $C_{2,s}$ and $C_{3,s}$ are the concentrations of solutes in brine in direct contact with the mushroom; $\partial/\partial n$ is the normal derivative operator. Bi is the Biot number, which expresses the ratio between internal and external mass transfer resistance and has a relationship with the coefficients h_m and λ_m (equation 14):

$$Bi = \frac{h_m R_i}{\lambda_m}, \quad i = 1, 2, 3 \quad (14)$$

where R_i is the characteristic dimension that corresponds to the *x*-axis half distance.

Porosity determination by X-ray computed microtomography (μ-CT)

μ-CT porosity assays were performed using the X-ray computed microtomography (Skyscan 1173, Bruker, Kontich, Belgium). The μ-CT used various radiographs taken at specific angular steps to build the 3D image of the sample by stacking multiple 2D sections. Thus, the total porosity (open porosity + closed porosity) and pore size distributions of the sample were determined. The spatial resolution was 12.5 μm.

For this assay, pre-cooked whole mushrooms of approximately 10 g with a moisture content of 91.95 ± 0.85% were used. The percentage of empty pores was calculated in the entire sample.

Statistical test, adjustment of the diffusion coefficients and Biot number

It was necessary to provide the input values of the main and cross coefficients as well as the Biot number for the software simulate the mass transfer and calculate the concentrations of salts in each time and position. These values were adjusted using the super modified simplex optimization method,[24] associated with the desirability functions.[25] Then an optimization algorithm[24] proposed combinations for the Biot number and the main and cross diffusion coefficients. These combined values proposed were evaluated through the FEM method. Through the statistical test,[15] the simulated concentrations of NaCl, KCl and Fe^{2+} were compared to the experimental results applying equation 15. The percentage errors found were evaluated using the optimization method, giving new value combinations, in order to minimize the error between simulated and experimental values. This procedure was repeated until the calculated values for the errors, main and cross diffusion coefficients and Biot number were stabilized.

$$\text{Error}(\%) = 100\sum_{i=1}^{N}\left[\frac{\left|\underline{C}_{calc} - \underline{C}_{exp}\right|}{\underline{C}_{exp}}\right]\frac{1}{N} \quad (15)$$

where: $\underline{C}_{calc}$ is the average concentration estimated by the numerical solution; $\underline{C}_{exp}$ is the average experimental concentration and N is the number of observations considered.

Results and Discussion

Some parameters involving the adsorption of Fe^{2+} in the mushroom were determined prior to the simulations/optimization of diffusion coefficients and Biot number. Figure 1 shows the microtomography of the mushroom. It was observed that only 2.56% of the sample had empty pores, with 1.42% of these pores being closed and 1.14% open. On average, the mushroom used presented 91.95% of the volume occupied by water, occluded in the biosolid matrix. Therefore, the sum of empty and water-saturated pores shows a porosity of 94.51% in the mushroom. Oikonomopoulou and Krokida,[26] using a helium gas pycnometer, obtained a value of 94.70% for the lyophilized mushroom.

Figures 2 and 3 show the fits of the Langmuir and Freundlich isotherms in the linearized form to the experimental data. It can be noted that the linearized form of the Langmuir isotherm satisfactorily fitted the experimental data, with a minimum coefficient of determination of 0.9933. The adsorption constant (K_L) and maximum adsorption capacity (q_m) of the Langmuir isotherm, determined by the least square method of the experimental data, and used in the computer simulations, were equal to 0.0188 L mg^{-1} and 1.049 mg g^{-1}, respectively. The adsorption constant plays a fundamental role in mass transfer, since it gives the adsorption affinity of Fe^{2+} in the active sites of the mushroom.

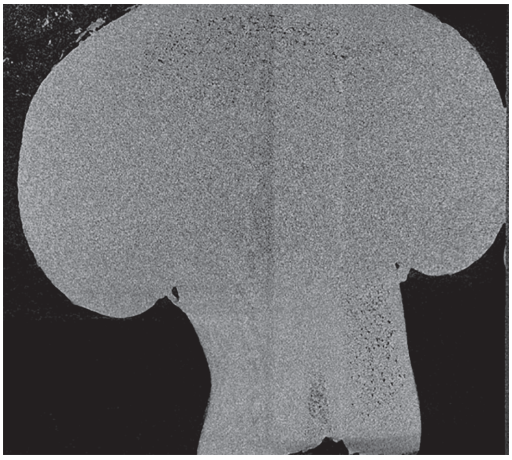

Figure 1. Interior microtomography (μ-CT) of the precooked mushroom (SkyScan 1173, 1 pixel = 12.5 μm).

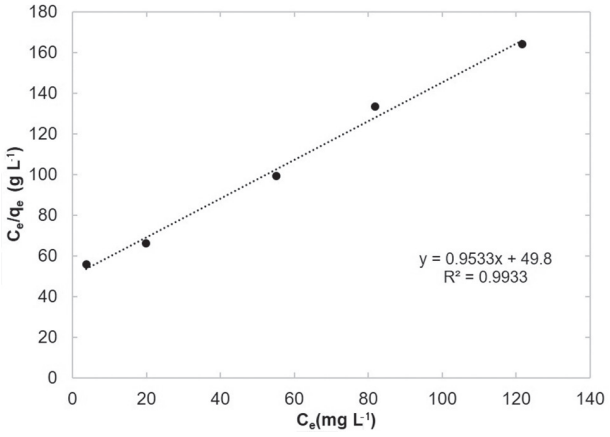

Figure 2. Linear model fit of the Langmuir isotherm.

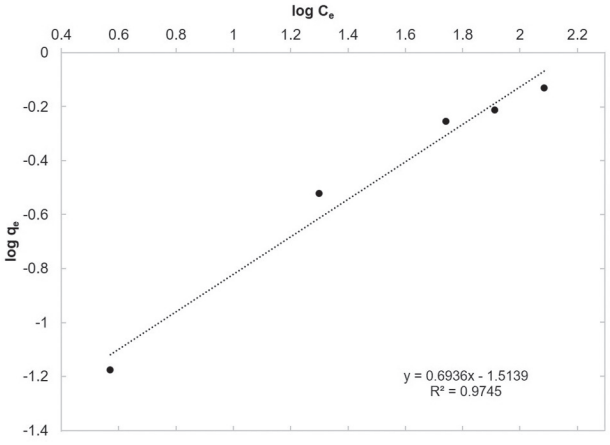

Figure 3. Linear model fit of the Freundlich isotherm.

The Langmuir model equation assumes that adsorption occurs by the formation of a single layer on the adsorbent surface, where adsorbate molecules are adsorbed to completely fill the adsorption sites that constitute the adsorbent surface. Furthermore, it considers that there is equivalence between the adsorption sites, uniform surface, and that the ability of a molecule to be adsorbed is independent of the filling of the adjacent sites, i.e., there is an independence between the sites.[20,27]

The optimization method started from a flat figure of 11 vertices, with the lower and upper limits of each parameter, based on literature[17] data and preliminary tests. The optimization algorithm suggested combinations between the diffusion coefficients and the Biot number (variables) that were used in the software simulations resulting in concentrations of the three ions which were compared with the experimental concentrations. The iterative method was kept until the smallest error was reached, and the suggested values for the Biot number and the cross and main coefficients remained stable.

The joint stabilization of the 10 variables occurred from the simplex number 35. The percentage errors of each species when considering 79 h of mass transfer process were from 3.11 to 15.34% (Table 1).

Table 1. Percentage errors of each specie after stabilization

	Percentage error / %		
	Na^+	K^+	Fe^{2+}
Static brine	5.66	5.36	8.26
Stirred brine	3.11	3.30	15.34

Regarding the mathematical modeling, the percentage error values for Fe^{2+} can be considered acceptable. Angilelli *et al.*,[18] Galvan *et al.*,[16] and Ferrari and Hubinger[28] reported percentage error values of up to 11.24, 16.96 and 25.00%, respectively.

The optimal values obtained as well as the film coefficients, determined from the values of the Biot number and the main and cross diffusion coefficients (equation 14), can be observed in Table 2.

Diffusion coefficients are the same for static and stirred systems because they refer to mass transfer within the biosolid. Biot number, maximum capacity and adsorption constant of the ferrous ion, in the stirred system, were determined by estimation.

The values of diffusion coefficients for the studied components were expected, because the ion mobility is related to the hydration radius. Potassium, sodium and iron have ionic radius of 151, 118 and 92 pm, with coordination number 8,[29] and the smaller the ionic radius the higher the affinity for water, and therefore the greater the hydrated radius.[30] For this reason, the iron ion has the value of the diffusion coefficient lower than sodium and potassium.

In addition, it was found that the values of the principal diffusion coefficients of sodium is almost double, and

Table 2. Cross and main diffusion coefficients, Biot number and mass transfer coefficient

		Na^+	K^+	Fe^{2+}
Main diffusion coefficient / (m^2 s^{-1})		4.567×10^{-10} (D_{11})	7.886×10^{-10} (D_{22})	1.943×10^{-10} (D_{33})
Cross diffusion coefficient / (m^2 s^{-1})		0.571×10^{-10} (D_{12})	0.609×10^{-10} (D_{21})	0.0021×10^{-10} (D_{31})
		0.588×10^{-10} (D_{13})	0.473×10^{-10} (D_{23})	0.0023×10^{-10} (D_{32})
Static brine	h_m / (m s^{-1})	2.049×10^{-6}	3.209×10^{-6}	0.708×10^{-6}
	Biot number[a]		56.37	
Stirred brine	h_m / (m s^{-1})	5.0163×10^{-6}	7.858×10^{-6}	1.7326×10^{-6}
	Biot number[a]		138	

[a]Biot number estimated in relation to the *x*-axis. D_{11}, D_{22}: main diffusion coefficients of NaCl and KCl, respectively; D_{33}: effective diffusion coefficient of iron; D_{12}, D_{21}, D_{31}, D_{13}, D_{23}, D_{32}: cross-diffusion coefficients; h_m: mass transfer coefficient.

for potassium almost triple, when compared to the work of Bordin *et al.*,[17] in which pre-cooked mushroom was immersed in brine with 3% of salt (70% NaCl and 30% KCl) and determined the main diffusion coefficients of 2.692×10^{-10} and 2.953×10^{-10} m^2 s^{-1} for sodium and potassium, respectively.

The presence of Fe^{2+} in the brine may have influenced the increase in diffusion coefficient values. This happens because iron is a transition metal and forms many complexes in the empty sites of porous mushroom matter, which consequently decrease the weak interactions of sodium and potassium ions with chemical constituents in the biosolid matrix. Furthermore, the presence of iron ion in the brine alters the ionic strength of the mixture.

The cross coefficients are considerably smaller than the main ones, which is expected because diffusion relative to the gradient is more important than the cross diffusion.[17,18] However, the value of the cross-diffusion coefficient favors an increase in the mass transfer coefficient, indicating that the ions find lower mobility resistance at the brine-mushroom interface.

The interference of sodium on potassium flow, and *vice versa*, practically cancel each other because the values of the cross coefficients are close (Table 2). In iron flow, sodium and potassium interferences predominate, since iron has a small interference in the sodium and potassium fluxes.

The experiments with and without stirring were performed to show the importance of mass transfer resistance (Figures 4 and 5). According to Bona *et al.*,[15] when the value of the Biot number is equal to or greater than 100, the internal resistance is limiting, and as this value decreases, the external resistance increases, showing the interference of a physical barrier on the solid surface contours.[31]

The Biot number for solute transfer in static brine was 56.37, which indicates the interference of a film formed on the mushroom surface contours. The Biot number was 138 in the stirring brine.

The reduction in mass transfer resistance is also verified by increasing the film transfer coefficient of the ions. In stirred brine this value was 2.45, higher than in static brine, showing that the degree of system disturbance decreased the resistance of the formed film and thus facilitated the mobility of ions at the solution/mushroom interface.

Figure 4 shows the diffusion profile of the simulated and experimental concentrations, with the optimized values

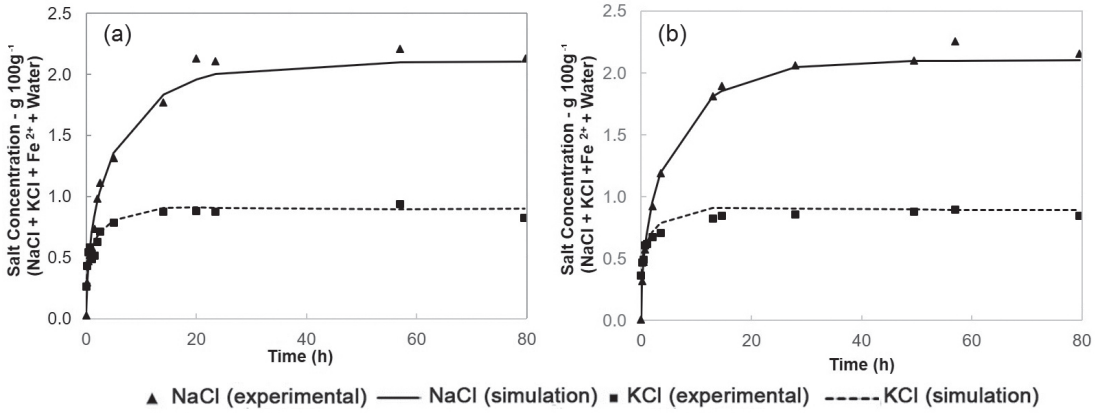

Figure 4. Diffusion profile of simulated and experimental NaCl and KCl salts over time in (a) static and (b) stirred brine.

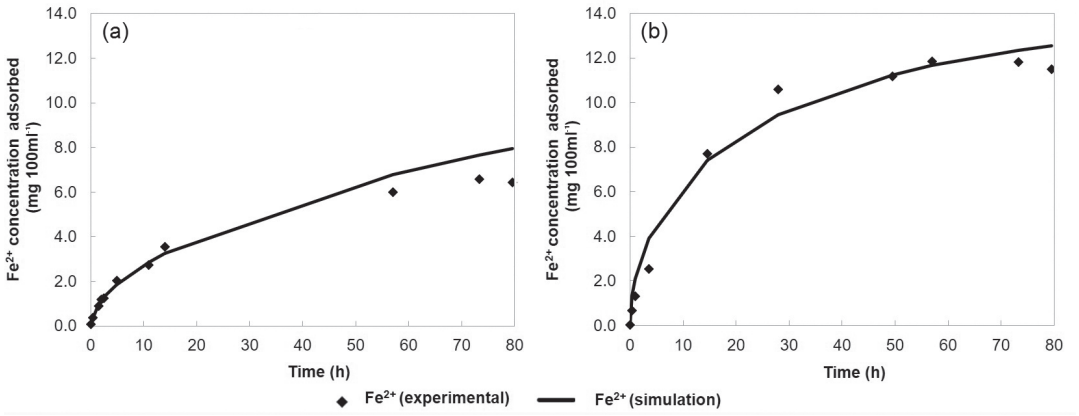

Figure 5. Profile of experimental and simulated adsorbed Fe^{2+} concentrations *per* 10 g mushroom in 100 mL of brine (NaCl + KCl + Fe^{2+} + water) over time, in (a) static and (b) stirred brine.

of the Biot number, cross and main diffusion coefficients, for stirred and static salting over time.

Figure 4 shows that the beginning of stabilization of sodium chloride concentrations started in the 20 h, and the potassium chloride stabilization started in the 4 h. This behavior was observed in both systems.

Figure 5a shows that the diffusion and adsorption of Fe^{2+} in the mushroom immersed in the static brine stabilized after 55 h, in which it adsorbed 46.43% (6.5 mg) of the solution solute. Figure 5b, in stirred brine, the mushroom adsorbed 81.28% (11.38 mg) and reached equilibrium starting in the 28 h. In the mathematical model for the stirred system a maximum adsorption capacity of 1.15 mg g^{-1} was estimated and the Langmuir adsorption constant was 0.0013 L mg^{-1}.

Figures 6 and 7 show the simulated distribution profiles of the NaCl and KCl salts along the *z*-axis of the sample, in static and stirred systems, at 50 and 20 h, respectively. They show that in the first hours of simulation, in the stirred system, concentrations at the edges of the mushroom quickly reach the boundary conditions established by equations 11-13. Considering the static system, the boundary condition no longer occurs accurately due to the formation of a film at the thicker interface.

The Na^+ equalization time inside the mushroom was 50 h (Figure 6), and no difference was observed between the stirred and static system. For K^+ ion the equalization time for the static system was 15 h (Figure 7a) and for the stirred was 12 h (Figure 7b). The equalization time difference for the static and stirred system was 3 h. However, when compared with the values obtained by Bordin *et al.*,[17] the equilibrium time for the system stirred was 80 h for NaCl and 35 h for KCl. Therefore, the presence of iron in the brine influenced the mobility of sodium and potassium ions into the mushroom.

Applying the finite element method, it was possible to simulate and verify the iron ion distribution inside the champignon mushroom sample, during the static and stirred brine mass transfer process in the time of 79.58 h (Figures 8a and 8b). In the center of the mushroom (light region), a lower iron concentration of

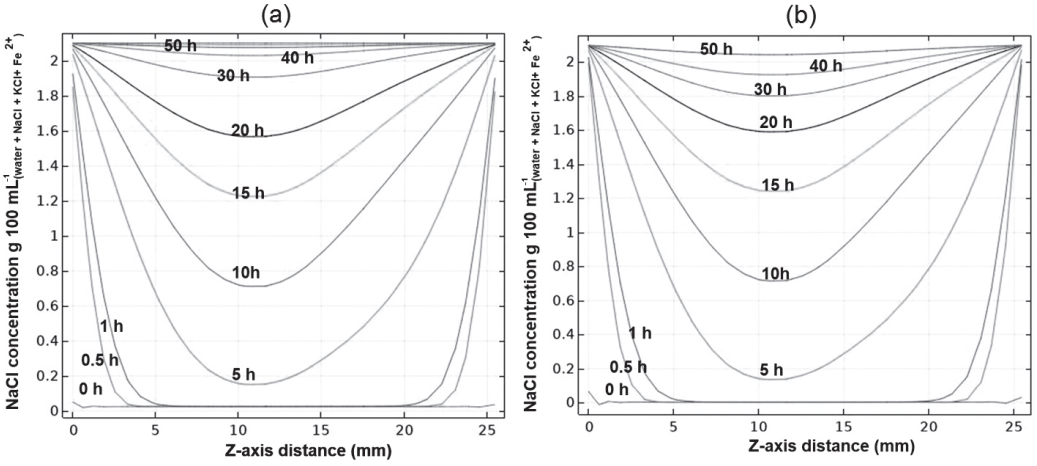

Figure 6. Distribution profile in the *z*-axis of mushroom NaCl concentration, in (a) static and (b) stirred brines, over a period of up to 50 h of salting, obtained by simulation.

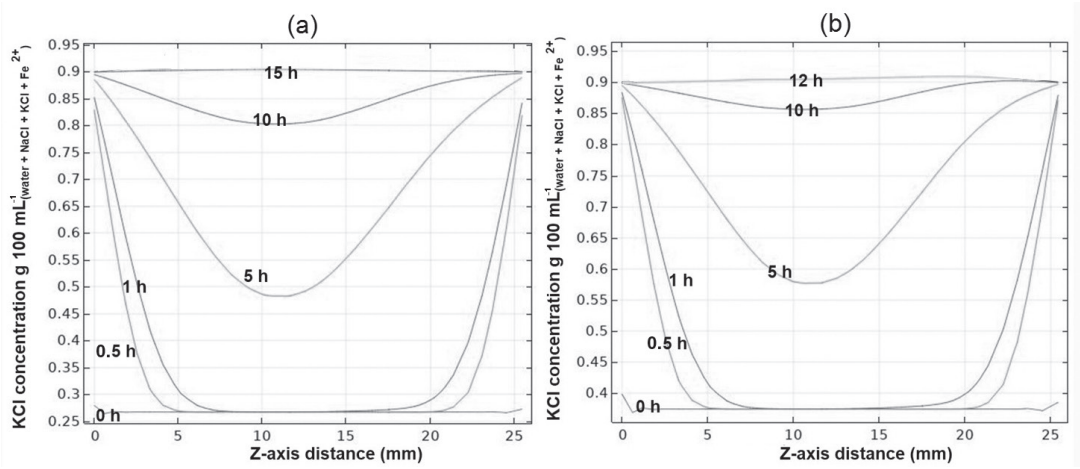

Figure 7. Distribution profile in the *z*-axis of mushroom KCl concentration, in (a) static and (b) stirred brines, over a period of up to 20 h of salting, obtained by simulation.

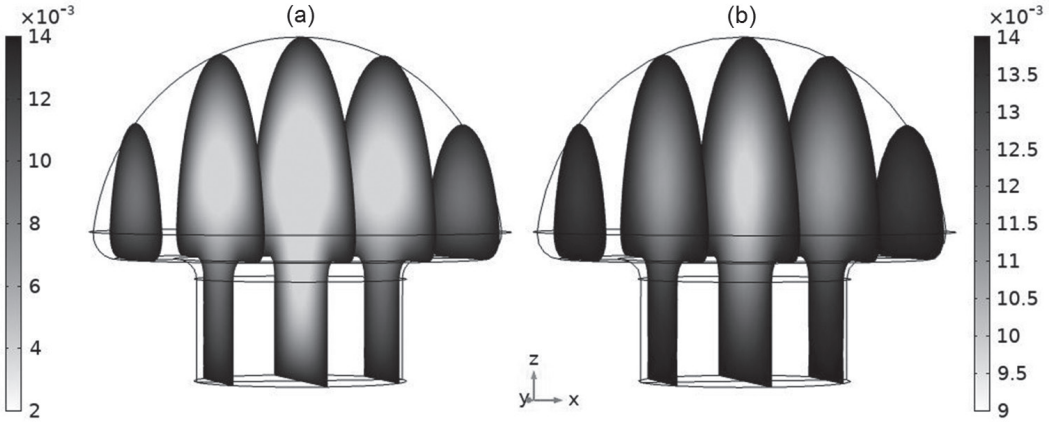

Figure 8. Distribution profile of Fe^{2+} concentrations (g 100 mL^{-1}) in the mushroom after 79.58 h of simulation of the transfer process in (a) static and (b) stirred brine.

0.002 g 100 $mL^{-1}_{(water + NaCl + KCl + Fe^{2+})}$ in the static system, and 0.009 g 100 $mL^{-1}_{(water + NaCl + KCl + Fe^{2+})}$ in the stirred system were observed. However, near the edges of the mushroom, it has been observed a higher concentration of such ion, mainly under stirred system. Thus, the hydrodynamic condition of the stirred Fe^{2+} system affected the external resistance of the adsorbent as the mass transfer through the film increased. Therefore, the Biot number equal to 138 (Table 2) shows that internal resistance is limiting, i.e., pore mass transfer becomes predominant.[17]

Conclusions

The mathematical model with the simplex optimization allowed the study and the determination of the main, cross and film coefficients in the transfer process of Na^+, K^+ and Fe^{2+} ions in champignon mushroom in static and stirred brines.

The Biot number obtained in the static brine indicated the formation of a stationary film at the mushroom interface and solution, on the other hand by stirring the brine it was possible to increase the value of the film coefficient, and consequently decreases the external resistance by facilitating the entry of ions on the mushroom surface, mainly for diffusion and adsorption of ferrous ion.

Acknowledgments

The authors would like to thank the State University of Londrina (UEL) for the technical support, the X-ray Technique Analysis Laboratory (LARX) and CAPES for the scholarship granting.

Author Contributions

Mirian S. P. Bordin was responsible for conceptualization, formal analysis, investigation, methodology, software, validation, visualization and writing: review and editing; Hágata Cremasco, Diego Galvan and Evandro Bona for the methodology, software and writing: review and editing;

Marco A. J. Clemente for the methodology and software; Ana Carolina G. Mantovani for the methodology, writing: original draft, review and editing; Dionisio Borsato for the funding acquisition, methodology, project administration, software, supervision and writing: review and editing.

References

1. Bryszewska, M. A.; Tomás-Cobos, L.; Gallego, E.; Villalba, M.; Rivera, D.; Saa, D. L. T.; Gianotti, A.; *LWT - Food Sci. Technol.* **2019**, *99*, 431.
2. Torres-Fuentes, C.; Alaiz, M.; Vioque, J.; *Food Chem.* **2012**, *134*, 1585.
3. Wang, S.; Ouerdane, L.; Hoekenga, O.; Szpunar, J.; Lobinski, R.; *Food Chem.* **2019**, *294*, 414.
4. Caetano-Silva, M. E.; Alves, R. C.; Lucena, G. N.; Frem, R. C. G.; Bertoldo-Pacheco, M. T.; Lima-Pallone, J. A.; Netto, F. M.; *Food Res. Int.* **2017**, *101*, 73.
5. Caetano-Silva, M. E.; Bertoldo-Pacheco, M. T.; Paes-Leme, A. F.; Netto, F. M.; *Food Res. Int.* **2015**, *71*, 132.
6. Regula, J.; Krejpcio, Z.; Staniek, H.; *J. Med. Food* **2010**, *13*, 1189.
7. Reis, F. S.; Barros, L.; Martins, A.; Ferreira, I. C. F. R.; *Food Chem. Toxicol.* **2012**, *50*, 191.
8. Reis, F. S.; Martins, A.; Vasconcelos, M. H.; Morales, P.; Ferreira, I. C. F. R.; *Trends Food Sci. Technol.* **2017**, *66*, 48.
9. Bach, F.; Helm, C. V.; Bellettini, M. B.; Maciel, G. M.; Haminiuk, C. W. I.; *Int. J. Food Sci. Technol.* **2017**, *52*, 2382.
10. Albarracín, W.; Sánchez, I. C.; Grau, R.; Barat, J. M.; *Int. J. Food Sci. Technol.* **2011**, *46*, 1329.
11. Harkouss, R.; Chevarin, C.; Daudin, J.-D.; Sicard, J.; Mirade, P.-S.; *J. Food Eng.* **2018**, *218*, 69.
12. Feltrin, A. C.; de Souza, V. R.; Saraiva, C. G.; Nunes, C. A.; Pinheiro, A. C. M.; *Int. J. Food Sci. Technol.* **2015**, *50*, 730.
13. Barat, J. M.; Baigts, D.; Aliño, M.; Fernández, F. J.; Pérez-García, V. M.; *J. Food Eng.* **2011**, *106*, 102.
14. Armenteros, M.; Aristoy, M. C.; Barat, J. M.; Toldrá, F.; *Food Chem.* **2009**, *117*, 627.
15. Bona, E.; Carneiro, R. L.; Borsato, D.; Silva, R. S. S. F.; Fidelis, D. A. S.; Silva, L. H.; *Braz. J. Chem. Eng.* **2007**, *24*, 337.
16. Galvan, D.; Chendynski, L. T.; Mantovani, A. C.; Quadri, M.; Killner, M.; Cremasco, H.; Borsato, D.; *J. Braz. Chem. Soc.* **2020**, *31*, 313.
17. Bordin, M. S. P.; Borsato, D.; Cremasco, H.; Galvan, D.; Silva, L. R. C.; Romagnoli, É. S.; Angilelli, K. G.; *Food Chem.* **2019**, *273*, 99.
18. Angilelli, K. G.; Orives, J. R.; da Silva, H. C.; Coppo, R. L.; Moreira, I.; Borsato, D.; *J. Food Process. Preserv.* **2015**, *39*, 329.
19. Gomes, C. A. O.; Silva, F. T.; *Recomendações Técnicas para o Processamento de Conservas de Cogumelos Comestíveis*; Embrapa Agroindústria de Alimentos: Rio de Janeiro, Brazil, 2000. Available at https://ainfo.cnptia.embrapa.br/digital/bitstream/item/34412/1/2000-DOC-0043.pdf, accessed in December 2019.
20. Chen, Y.; Zhang, W.; Zhao, T.; Li, F.; Zhang, M.; Li, J.; Zou, Y.; Wang, W.; Cobbina, S. J.; Wu, X.; *Food Chem.* **2016**, *194*, 712.
21. Febrianto, J.; Kosasih, A. N.; Sunarso, J.; Ju, Y.-H.; Indraswati, N.; Ismadji, S.; *J. Hazard. Mater.* **2009**, *162*, 616.
22. *COMSOL Multiphysics®*, version 5.2; COMSOL, Inc., Burlington, MA, USA, 2016.
23. Onsager, L.; *Ann. N. Y. Acad. Sci.* **1945**, *46*, 241.
24. Bona, E.; Borsato, D.; Silva, R.; Herrerra, R.; *Acta Sci.* **2000**, *22*, 1201.
25. Derringer, G.; Suich, R.; *J. Qual. Technol.* **1980**, *12*, 214.
26. Oikonomopoulou, V. P.; Krokida, M. K.; *Drying Technol.* **2012**, *30*, 351.
27. Langmuir, I.; *J. Am. Chem. Soc.* **1918**, *40*, 1361.
28. Ferrari, C. C.; Hubinger, M. D.; *Int. J. Food Sci. Technol.* **2008**, *43*, 2065.
29. Atkins, P. W.; Shriver, D. F.; *Shriver & Atkins Inorganic Chemistry*, 4th ed.; Oxford University Press: Oxford, 2006.
30. Lee, J. D.; *Concise Inorganic Chemistry*, 5th ed.; Chapman & Hall: London, UK, 1996.
31. Rakotondramasy-Rabesiaka, L.; Havet, J.-L.; Porte, C.; Fauduet, H.; *Sep. Purif. Technol.* **2010**, *76*, 126.

Submitted: September 11, 2019
Published online: December 19, 2019

This is an open-access article distributed under the terms of the Creative Commons Attribution License.